Validation of a Simulated Dose Reduction Methodology Using Digital Mammography CDMAM Images and Mastectomy Images

Mary Yip[1], Federica Zanca[2], Alistair Mackenzie[3], Adam Workman[4], Kenneth C. Young[3], David R. Dance[3], Hilde Bosmans[2], Emma Lewis[1], and Kevin Wells[1]

[1] Centre for Vision, Speech and Signal Processing, Faculty of Engineering and Physical Sciences, University of Surrey, Guildford, GU2 7XH, UK
m.yip@surrey.ac.uk
[2] Department of Radiology, University Hospitals Gasthuisberg, Herestraat 49, B-3000 Leuven, Belgium
[3] National Coordinating Centre for the Physics of Mammography, Royal Surrey County Hospital, Guildford, GU2 7XX, UK
[4] Northern Ireland Regional Medical Physics Agency, Forster Green Hospital, Belfast, BT8 4HD, UK

Abstract. The purpose of this study is to evaluate the effect of simulated dose reduction using CDMAM and mastectomy images acquired on two digital mammography systems. High dose images have been artificially degraded to reduced dose levels by systematically adding filtered noise. Automated scoring has been carried out on the degraded CDMAM images and on experimental CDMAM images, taken at the same corresponding reduced doses. Contrast-detail curves were derived for both, at all doses, and compared. Relative difference in the contrast-detail curves was approximately 5% overall for all four doses.

For the mastectomy images noise power spectra were obtained and the ratio of experimental to synthetic low dose NPS profiles averaged for all doses at 1.04. The largest differences in the NPS profiles were found at the high spatial frequencies, corresponding with the differences in the small discs in the contrast-detail curves.

Keywords: Digital mammography, simulation, CDMAM phantom, validation, mastectomy, dose reduction.

1 Introduction

There is a growing interest in image simulation in digital radiography, and in mammography in particular[1,2,3,4,5,6]. Image simulation provides a means to optimise digital mammography systems for improved breast cancer detection. Image simulation studies could make clinical trials more targeted as simulation studies can be used to study some effects in advance.

Recently, there has been focus on the effect of reducing dose levels in digital mammography images upon detection of mammographic lesions[1,2]. Results

J. Martí et al. (Eds.): IWDM 2010, LNCS 6136, pp. 78–85, 2010.

indicate that dose could be reduced with little detriment to the detection of masses. However, the task of microcalcification detection appeared to have significantly greater dependence on the increased relative noise in the images. This is because breast structure noise dominates when trying to detect relatively large objects such as masses but detector noise is important for the detection of small details such as microcalcifications. In contrast-detail tasks such as scoring of images of the CDMAM phantom, there is a direct link between increasing dose and the detection of small details[7]. This study aimed to validate a method to simulate reduced radiation dose in digital mammograms. The same methodology is applied to mastectomy images for further analysis with use of spectral analysis[8,9].

2 Methodology

2.1 Materials

Sixteen images of the CDMAM (version 3.4) were acquired at each of five doses using the Hologic Selenia system with the CDMAM phantom placed between two slabs of PMMA 2cm thick. The images acquired at the highest dose (31kVp Mo/Rh, 5.91mGy mean glandular dose) were used as the reference images for the subsequent synthesised low dose images (0.34, 0.80, 1.48, 2.95mGy MGD). Flat field images for 5cm of PMMA were acquired at the same beam quality, exposure settings and setup as the CDMAM images. Detector response and NPS measurements were carried out on these flat field images and used for the dose reduction methodology.

Four sets of mastectomy images were acquired on the Siemens Novation system. Each mastectomy sample was placed on the breast support and compressed. The mastectomy sample was exposed with the tube voltage held constant whilst the tube current time product was varied. Care was taken not to move the mastectomy sample after each exposure. The highest dose mastectomy image was used as the reference image for synthesizing subsequent lowered dose images. Table 1 shows the doses used for each mastectomy set as well as their compressed thicknesses. Flat field images using three and five centimetres of PMMA was used in the same setup as the mastectomy samples for detector response and NPS measurements to be used with the dose reduction methodology. Note that all images used in this study are raw and unprocessed.

2.2 Dose Reduction

Båth et al's methodology[10], which had been previously applied to chest X-ray images, has now been implemented for the first time to degrade the following experimentally acquired mammography images: CDMAM and mastectomy images. Furthermore, the NPS was modelled to three noise sources: electronic, quantum and structural. Firstly, the linearised pixel intensity values of the original image, $I_o(x, y)$, were scaled by a ratio of the dose to be simulated, D_{sim}, to the original

Table 1. Beam quality (W = Tungsten, Rh = Rhodium, Mo = Molybdenum), Tube current time product and mean glandular dose settings for each mastectomy sample set. Doses in brackets denote the highest dose image from which the other low dose images were derived.

Set	Beam Quality	Tube Current time product (mAs)	Mean Glandular Dose (mGy)	Compressed Breast Thickness (mm)
1	29 W/Rh	28, 57, 110 (220)	0.3, 0.7, 1.4 (2.7)	50
2	29 W/Rh	10, 20, 50, (68)	0.1, 0.2, 0.4 (0.8)	50
3	25 Mo/Rh	10 (61)	0.2 (1.3)	30
4	25 Mo/Rh	20, 34, 45 (199)	0.4, 0.7, 1.0 (4.3)	30

dose of the image, D_o, to give the original scaled image, $I_{o,sc}$. NPS was measured for each dose level and fitted to each point in the NPS array against detector air kerma, K:

$$NPS_{tot}(u,v) = NPS_e(u,v) + NPS_q(u,v).K + NPS_s(u,v).K^2 \tag{1}$$

where NPS_{tot}, NPS_e, NPS_q and NPS_s are the total, electronic, quantum and structure noise sources, respectively.

Structural noise scales with the dose correction, therefore only electronic and quantum noise images were created. Noise images were created to account for the difference in noise level and frequency content between the $I_{o,sc}$ and that expected for a lower dose image, D_{sim}. This was undertaken through the use of a frequency-based noise transfer function, NTF, equal to the square root of the difference of the NPS between the two images, I_{sim} and $I_{o,sc}$, for each noise source and applied to Gaussian noise images.

$$I_N(x,y) = FT^{-1}(NTF(u,v).(FT(I_G(x,y)))) \tag{2}$$

where

$$NTF(u,v) = \sqrt{\frac{NPS_{sim}(u,v) - NPS_{o,sc}(u,v)}{NPS_{sim}(0,0) - NPS_{o,sc}(0,0)}} \tag{3}$$

For the quantum noise, the difference in NPS_q for the I_o, sc and I_{sim} was applied to equation 2. Both noise sources were scaled on a pixel-by-pixel basis as shown:

$$\begin{aligned} I_{sim}(x,y) = I_{o,sc}(x,y) &+ \left[k_e.I_{N,e}(x,y).\left(1 - (D_{sim}/D_{orig})^2\right)\right] \\ &+ [k_Q.(I_{o,sc}(x,y))^n.I_{N,Q}(x,y)] \end{aligned} \tag{4}$$

where k_e, k_Q and n are coefficients to be fitted. n was found to be 0.5 ± 0.03 for both systems and settings implemented in this study.

This method was then applied to derive synthetically dose-reduced CDMAM and mastectomy images. For degrading CDMAM images the highest

dose (5.91mGy MGD) CDMAM image was used as the reference image from which low dose images (0.34, 0.80, 1.48, 2.95mGy MGD) were subsequently obtained. All experimentally acquired CDMAM images were scored with an automated scoring tool (CDCOM[11]) and contrast-detail curves derived for each dose as outlined in [12]. The same procedure was repeated for the synthesized dose reduced CDMAM images and compared with the experimentally acquired counterparts.

The dose reduced mastectomy images were compared, quantitatively and visually, with their experimentally acquired counterparts. In addition, noise power spectra[8,9] were measured in the same region of interest for each dose for the simulated and experimental mastectomy images and the profiles compared. To ensure the same region was analysed in each image and that results were not affected by any slight movement of the mastectomy sample, the mastectomy images were checked for alignment. In addition, NPS analysis was undertaken within the central portion of the mastectomy samples to ensure uniform thickness was maintained in the region of interest.

3 Results

Figure 1 show the normalised NPS profiles of high dose flat-field images and the dose reduced flat-field images for the Hologic and Siemens Novation systems. For the Hologic system, there was a relative difference between the experimental and synthetic low dose shown of approximately 4.7% averaged across the radial averaged NNPS. For the Siemens Novation system, there was a relative difference between the experimental and sythetic low dose shown of 2.7%.

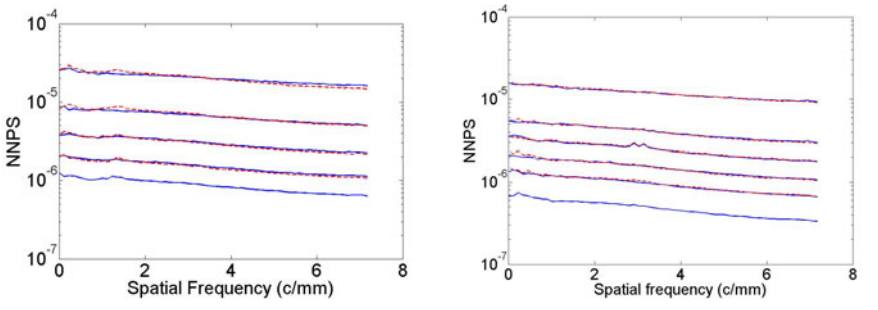

(a) (b)

Fig. 1. (a)Normalised NPS profiles for Hologic system. NNPS curves are given for (from top down) 0.34, 0.80, 1.48, 2.95 and 5.91mGy MGD. (b) NNPS profiles for the Siemens Novation. NNPS curves are given for (from top down) 0.2, 0.4, 0.7, 1.0, 1.3 and 4.3mGy MGD. Experimental data is shown in solid blue whilst the synthetic data is shown in the dashed red curve.

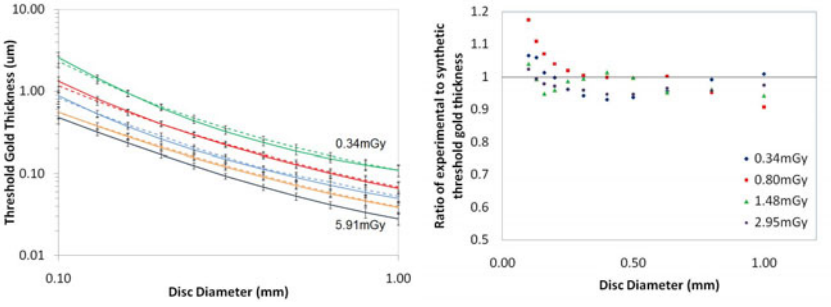

(a) (b)

Fig. 2. (a)Contrast detail curves obtained from experimentally acquired CDMAM images at different doses (solid curves) and the simulated reduced dose CDMAM images (dashed curves). Four doses (0.34, 0.80, 1.48, 2.95mGy MGD, from top down) were simulated from the highest dose of 5.91mGy. Error bars denote two standard error means.

3.1 CDMAM Images

Figure 2 shows the contrast detail curves obtained for the experimental and dose-reduced CDMAM images. The dashed curves denote the fitted predicted human threshold contrasts[12] for the synthetic data. The noise added synthetically have led to the contrast details curves to maintain the gradient of the original high dose result, whilst shifting up with increasing relative noise in the image as expected. All the synthetic data curves are similar to that of the experimentally acquired and error bars indicate they are within range of each other. A ratio of the experimental to synthetic results were found to be, across all discs, on average 0.97 for all doses as shown in Figure 2b. This shows that noise may have been overestimated in the synthetic images compared to the experimental CDMAM images.

3.2 Mastectomy Images

Figure 3 shows a region of one set of mastectomy images at 4.3 and 1.0mGy MGD for the experimental (Figure 3b) and synthetic (Figure 3c images, respectively. The appearance of the lesion (a mass with microcalcifications) in the region shown degrades dramatically as the dose was reduced down to one quarter of the high dose image. A profile of the experimental and synthetic images is also shown in Figure 3d, a difference of 1% was found between the profiles. Figure 4 shows the radially averaged noise power spectra for four mastectomy images sets, the settings of which are shown in Table 1. As the dose increased, the system noise increased as expected. NPS of the mastectomy images lead to a relative difference of 7% on average across all doses. The difference increased as the difference between the original dose and the dose to be simulated became greater. The largest difference between experimental and synthetic NPS was found at the higher spatial frequencies.

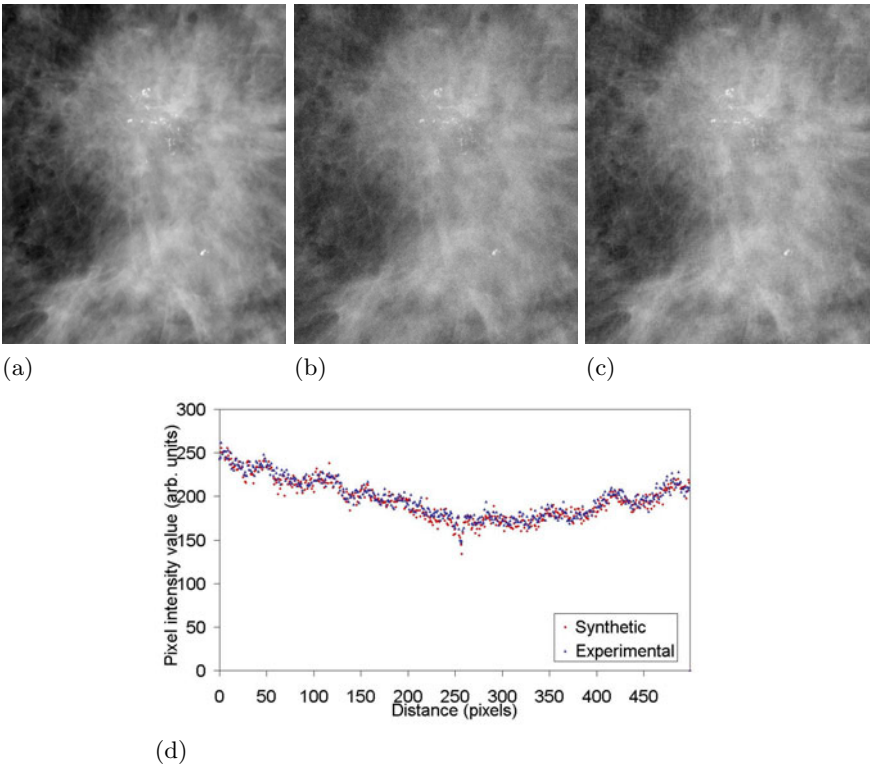

Fig. 3. (a) and (b) show the same cropped region of a mass with microcalcifications in a mastectomy sample acquired at 4.3 and 1.0mGy (MGD), respectively. (c) shows the mastectomy sample synthetically dose reduced from 4.3 to 1.0mGy. (d) shows the profiles taken across (b) and (c) to compare the experimentally acquired low dose image with the simulated low dose image.

4 Discussion

The contrast detail curves of the simulated dose reduced CDMAM images match well to that of the experimentally acquired images. The detection of smaller discs were inferior for the CDMAM images simulated at a very low dose compared with the CDMAM images experimentally acquired at the low dose. This suggests there may have been some overestimation of the noise to be added as the difference between the original and simulated doses increased.

For the mastectomy work, the simulation has visibly degraded the appearance of the lesions in the mastectomy images, similar to that acquired at lower doses. The noise power spectra measurement of the mastectomy samples at different doses have shown how the system noise increases whilst the shape of the underlying anatomical noise power remained. Larger discrepancies were found in the

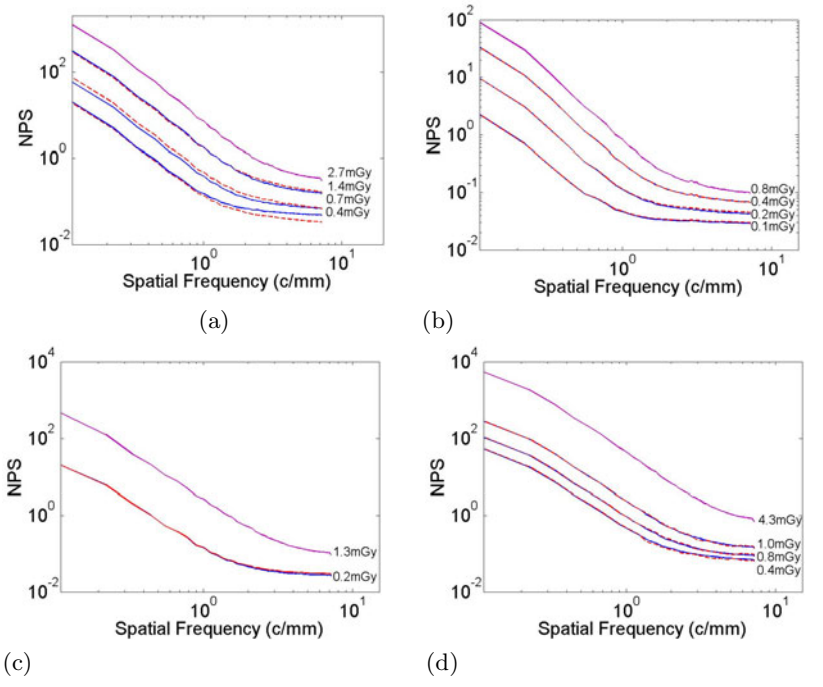

Fig. 4. (a – d) Radially averaged noise power spectra of a region in sets 1 – 4, respectively, of mastectomy images acquired at different doses and their synthetic counterparts. The dark curve represents the highest dose image from which the other low dose images were degraded from. Red dashed curves illustrates the NPS of synthetically degraded images whilst the blue solid curves show the NPS of their experimentally acquired counterparts.

higher spatial frequencies which corresponds to the poorer detection rates for the small discs in.

Despite reducing the dose to one quarter of the highest dose, the microcalcifications were still visible. However, the very fine calcifications became harder to discern as the relative noise increased in the low dose images. The work presented here shows raw images, thus affects from image processing packages have not been taken into account. Comparison of unprocessed and processed experimentally acquired mastectomy images showed a great difference in the image quality of microcalcifications for the high dose and low dose images. Further application of an image processing package on the synthetic images for further observer studies may be carried out in the future.

In conclusion, this work has validated a method to simulate reduced dose in mammography images, developing on Båth et al's work to incorporate other noise components. Such a method could be applied to study the effect of dose reduction on mass and/or microcalcification detection in clinical mammograms where optimal X-ray exposure factors may be deduced. This work could be

developed further to assess the effects of applying alternative beam qualities or even acquiring images of the same mastectomy sample with different detectors.

Acknowledgements. This work is part of the OPTIMAM project and is supported by the CR-UK & EPSRC Cancer Imaging Programme in Surrey, in association with the MRC and Department of Health (England).

References

1. Samei, E., Saunders, R.S., Baker, J.A., Delong, D.M.: Digital Mammography: Effects of Reduced Radiation Dose on Diagnostic Performance. Radiology 243(2), 396–404 (2007)
2. Ruschin, M., Timberg, P., Båth, M., Hemdal, B., Svahn, T., Saunders, R.S., Samei, E., Andersson, I., Mattson, S., Chakraborty, D.P., Tingberg, A.: Dose dependence of mass and microcalcification detection in digital mammography: Free response human observer studies. Med. Phys. 34(2), 400–407 (2007)
3. Saunders, R.S., Samei, E.: A method for modifying the image quality parameters of digital radiographic images. Med. Phys. 30(11), 3006–3017 (2003)
4. Workman, A.: Simulation of Digital Mammography. In: Flynn, M.J. (ed.) Medical Imaging 2005: Physics of Medical Imaging. SPIE, vol. 5745, pp. 933–942 (2005)
5. Zanca, F., Chakraborty, D.P., Van Ongeval, C., Jacobs, J., Claus, F., Marchal, G., Bosmans, H.: An improved method for simulating microcalcifications in digital mammograms. Med. Phys. 35(9), 4012–4018 (2008)
6. Grosjean, B., Muller, S.: Impact of Textured Background on Scoring of Simulated CDMAM Phantom. In: Astley, S.M., Brady, M., Rose, C., Zwiggelaar, R. (eds.) IWDM 2006. LNCS, vol. 4046, pp. 460–467. Springer, Heidelberg (2006)
7. Young, K.C., Oduko, J., Woolley, L.: Technical Evaluation of the Hologic Selenia Full Field Digital Mammography System. Technical Report from National Coordinating Centre for the Physics of Mammography (2007)
8. Bochud, F.O., Valley, J.-F., Verdun, F.R.: Estimation of the noisy component of anatomical backgrounds. Med. Phys. 26(7), 1365–1370 (1999)
9. Heine, J.J.: On the statistical nature of mammograms. Med. Phys. 26(11), 2254–2265 (1999)
10. Båth, M., Håkansson, M., Tingberg, A., Månsson, L.G.: Method of Simulating Dose Reduction for Digital Radiographic Systems. Radiation Protection Dosimetry 114(1-3), 253–259 (2005)
11. Visser, M., Karssemeijer, N.: Manual CDCOM version 1.5: software for automated readout of CDMAM 3.4 images, `http://www.euref.org`
12. Young, K.C., Cook, J.J.H., Oduko, J.M.: Automated and human determination of threshold contrast for digital mammography systems. In: Astley, S.M., Brady, M., Rose, C., Zwiggelaar, R. (eds.) IWDM 2006. LNCS, vol. 4046, pp. 266–272. Springer, Heidelberg (2006)